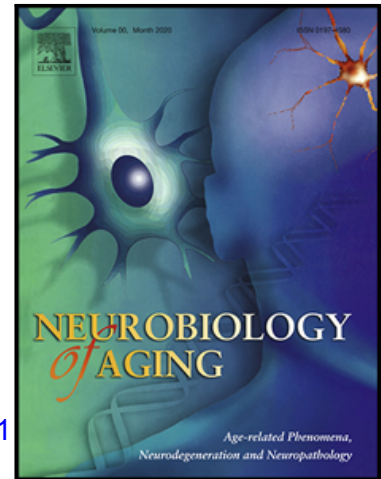# Journal Pre-proof

Genome-wide association study identifies susceptibility loci of brain atrophy to NFIA and ST18 in Alzheimer's disease

Bo-Hyun Kim , Kwangsik Nho , Jong-Min Lee , for the Alzheimer's Disease Neuroimaging Initiative

Please cite this article as: Bo-Hyun Kim , Kwangsik Nho , Jong-Min Lee , for the Alzheimer's Disease Neuroimaging Initiative, Genome-wide association study identifies susceptibility loci of brain atrophy to NFIA and ST18 in Alzheimer's disease, *Neurobiology of Aging* (2021), doi: https://doi.org/10.1016/j.neurobiolaging.2021.01.021

This is a PDF file of an article that has undergone enhancements after acceptance, such as the addition of a cover page and metadata, and formatting for readability, but it is not yet the definitive version of record. This version will undergo additional copyediting, typesetting and review before it is published in its final form, but we are providing this version to give early visibility of the article. Please note that, during the production process, errors may be discovered which could affect the content, and all legal disclaimers that apply to the journal pertain.

© 2021 Published by Elsevier Inc.

Highlights

- Genetic variants in *ST18* and *NFIA* are associated with cortical thickness in AD.

- A genetic variant in *ST18* is associated with severity of AD progression.

- *ST18* and *NFIA* are over-expressed in AD.

- Genetic variants in *ST18* and *NFIA* regulate expression levels of *ST18* and *NFIA*,

  respectively.

Highlights

- Genetic variants in *ST18* and *NFIA* are associated with cortical thickness in AD.

- A genetic variant in *ST18* is associated with severity of AD progression.

- *ST18* and *NFIA* are over-expressed in AD.

Genome-wide association study identifies susceptibility loci of brain atrophy to *NFIA* and *ST18* in Alzheimer's disease

Bo-Hyun Kim[1], Kwangsik Nho[2*], Jong-Min Lee[1*], for the Alzheimer's Disease Neuroimaging Initiative[§]

[1]Department of Biomedical Engineering, Hanyang University, Seoul, 04763, Korea

[2]Department of Radiology and Imaging Sciences, Indiana Alzheimer Disease Center, Indiana University School of Medicine, Indianapolis, IN, USA, 46202

[§]Data used in preparation of this article were obtained from the Alzheimer's Disease Neuroimaging Initiative (ADNI) database (adni.loni.usc.edu). As such, the investigators within the ADNI contributed to the design and implementation of ADNI and/or provided data but did not participate in analysis or writing of this report. A complete listing of ADNI investigators can be found at:

http://adni.loni.usc.edu/wp-

content/uploads/how_to_apply/ADNI_Acknowledgement_List.pdf

Correspondence to: Jong-Min Lee, PhD

Department of Biomedical Engineering, Hanyang University

Sanhakgisulkwan #319, Wangsimni-ro Seongdong-gu, Seoul, 04763, Korea

Email: ljm@hanyang.ac.kr

Correspondence may also be addressed to: Kwangsik Nho, PhD

Department of Radiology and Imaging Sciences, Indiana Alzheimer Disease Center, Indiana University School of Medicine, Indianapolis, IN, USA, 46202

Email: knho@iupui.edu

Abbreviations

ADNI = Alzheimer's Disease Neuroimaging Initiative; GWAS = genome-wide association study; MCI = mild cognitive impairment; CN = cognitive normal; SNP = single nucleotide polymorphism; FPKM = fragments per kilobase of transcripts per million mapped reads; CDR = clinical dementia rating; ROI = region of interest; IFGoperc.L = left inferior frontal gyrus, opercular part; IFGtriang. L= left inferior frontal gyrus, triangular part; ORBinf.L = left inferior frontal gyrus, orbital part; ORBsupmed. L= left superior frontal gyrus, medial orbital; ORBsupmed.R = right superior frontal gyrus, medial orbital; ACG.L = left anterior cingulate and paracingulate gyri; ACG.R = right anterior cingulate and paracingulate gyri; PCG.L = left posterior cingulate gyrus; PCG.R = right posterior cingulate gyrus; PHG.L = left parahippocampal gyrus; PHG.R = right parahippocampal gyrus; STG.L = left superior temporal gyrus; STG.R = right superior temporal gyrus; TPOmid.L = left temporal pole: middle temporal gyrus; TPOmid.R = right temporal pole: middle temporal gyrus; ITG. L= left inferior temporal gyrus; ITG.R = right inferior temporal gyrus; CNS= central nervous system

ABSTRACT

To identify genetic variants influencing cortical atrophy in Alzheimer's disease (AD), we performed genome-wide association studies (GWAS) of mean cortical thicknesses in 17 AD-related brain. In this study, we used neuroimaging and genetic data of 919 participants from the Alzheimer's Disease Neuroimaging Initiative cohort (ADNI), which include 268 cognitively normal controls (NC), 488 mild cognitive impairment (MCI), 163 AD individuals. A total of 3,041,429 single nucleotide polymorphisms (SNPs) were tested for association with cortical thickness. In addition, we evaluated whether GWAS-identified SNPs (single nucleotide polymorphism) have a correlation with gene expression levels within the brain tissues of humans. The results of GWAS indicated that rs10109716 in *ST18* (ST18 C2H2C-type zinc finger transcription factor) and rs661526 in *NFIA* (nuclear factor I A) genes are significantly associated with mean cortical thicknesses of the left inferior frontal gyrus and left parahippocampal gyrus, respectively. The rs661526 regulates the expression levels of *NFIA* in the substantia nigra and frontal cortex and rs10109716 regulates the expression levels of *ST18* in the thalamus. Furthermore, *ST18* is highly expressed in oligodendrocytes, which are the CNS (central nervous system) cells that produce myelin, and *NFIA* is highly expressed in astrocytes, which play an important role in the functioning and development of the brain. These results suggest a crucial role of identified genes for cortical atrophy and could provide further insights into the genetic basis of AD.

Keywords

1. Introduction

Alzheimer's disease (AD) is a common neurodegenerative disorder characterized by progressive loss of cognitive function and memory caused by neuronal dysfunction and death (Karch et al., 2014). The neurological hallmarks of AD include accumulation of senile plaques and neurofibrillary tangles, preceding the onset of clinical symptoms and contributing to clinical progression (Doraiswamy et al., 2014; Serrano-Pozo et al., 2011; Villemagne et al., 2013). AD has complex genetic etiology as well as environmental risk factors. The known risk factors of early-onset AD are three genes: *APP* (amyloid precursor protein), *PSEN1* (presenilin 1), and *PSEN2* (presenilin 2) (Bettens et al., 2013). For late-onset AD, *APOE* ε4 (Apolipoprotein E4) has become well known as one of the major genetic factors that increase the risk of AD. Recent genome-wide association studies (GWAS) identified more than 20 genes including *BIN1* (Bridging Integrator 1), *CLU* (Clusterin), and *CR1* (Complement C3b/C4b Receptor 1) that increase the risk of AD (Jun, 2010; Lambert et al., 2013; Wang et al., 2016). The heritability of AD is reported to be in the range of 60-80%; however, all the known AD-susceptibility genes, including *APOE,* explain only a small portion of genomic variance (Ridge et al., 2013). This is referred to as "missing heritability."

To address this problem, researchers have focused on GWAS with endophenotypes. Quantitative trait (also called endophenotypes) association studies have certain advantages over case-control studies. Traditional case-control GWAS designs that compare genotype frequencies between AD and control subjects require approximately 6,000 cases and 6000 controls to obtain 80% statistical power (Hirschhorn and Daly, 2005). Furthermore, case-control GWAS has problems concerning reliability and long-term stability of clinical diagnosis because diagnosis is based on behavioral characteristics and cognitive deficits that are typically difficult to quantify (Blanco-Gómez et al., 2016; Braskie et al., 2011; Wolthusen et al., 2015). Endophenotypes that are reliably measurable, stable, and continuously

distributed can improve the association studies by reducing the phenotype heterogeneity, and they can decrease the sample size required to achieve sufficient statistical power (Manchia et al., 2013; Meyer-Lindenberg and Weinberger, 2006; Potkin et al., 2009).

Endophenotypes that are heritable and disease-associated lie along the pathway between disease and genotypes. Several criteria have been proposed to identify valid endophenotypes: disease-associated, heritable, state-independent, co-segregates with disease within families, and present at a higher rate within affected families (Lenzenweger, 2013a), (Lenzenweger, 2013b).

A variety of endophenotypes have been established in AD. For example, endophenotypes for AD such as age at onset, memory, cognitive performance, and amyloid and tau accumulation have been used (E. et al., 2007; Gomez-Isla et al., 1996; Maxwell et al., 2018; Murphy et al., 1997; S. et al., 2008). Imaging genomics is an integrative research field that uses neuroimaging measures as endophenotypes and assesses the impact of genetic variation on neuroimaging measures. Brain structural atrophy such as hippocampal atrophy has been proposed as a marker for AD, and patterns of cortical atrophy have been shown to accurately track disease progression (Kale et al., 2019; Pini et al., 2016). Cortical thickness is one of the most sensitive biomarkers of cortical atrophy. Whole-brain mean cortical thickness as well as regional mean cortical thicknesses (e.g., inferior frontal, medial temporal, anterior and posterior cingulate) have been widely studied and found to be abnormally decreased in AD compared with cognitively normal controls (Dickerson et al., 2009; Du et al., 2007; Lerch et al., 2005; Querbes et al., 2009).

The genetic and non-genetic architecture of cortical thickness are complex. Although it is recognized that the thickness of the human cortex decreases with age (Shaw et al., 2016), environmental factors such as stress can also influence the cellular components that contribute to cortical thinning (Wong et al., 2018). Previous studies have reported that

cortical thinning is affected pathologically in AD. Studies of post-mortem tissue have shown that cortical thickness is reduced in regions of the cerebral cortex that are affected pathologically in AD. Cortical thinning is an indicator of the burden of neurofibrillary tangles and neuritic plaques, and it may also be a sign of loss of the neuronal, glial, or other important cellular components such as neuropil volume that are related to AD (Dickerson et al., 2009).

To identify the genetic architecture of cortical thickness in AD, we focused on mean cortical thicknesses of AD-associated cortical regions based on a reference study (Lerch et al., 2005). We selected 17 AD-associated ROIs (regions of interest) and performed GWAS. To investigate the functional role of genetic variants (Consortium et al., 2015), we performed expression quantitative trait locus (eQTL) analysis and differential expression analysis for GWAS-identified loci.

2. Materials and Methods

2.1 Study samples

All subjects were participants of the Alzheimer's Disease Neuroimaging Initiative (ADNI) including Alzheimer's disease (AD), mild cognitive impairment (MCI), and cognitively normal controls (CN) (Jack et al., 2008a; Susanne G Mueller et al., 2005; Susanne G. Mueller et al., 2005). Neuroimaging and genetic data of 940 participants were downloaded from the ADNI database (http://www.loni.ucla.edu/ADNI). Among them, 21 subjects failed at the MR image processing stage and were excluded from all the analyses. Demographics and genotypic characteristics of the final samples are listed in Table 1.

2.2 Image acquisition and processing

T1-weighted baseline MR images were downloaded from the ADNI database; MRI acquisition has been described previously (Jack et al., 2008b). Three-dimensional T1-weighted MRIs were processed using an automatic image analysis pipeline (CIVET) developed by the Montreal Neurological Institute. Briefly, we performed nonuniformity correction (Sled et al., 1998) and normalization to standard space using a linear transform (Collins et al., 1994). The registered MR images were classified into gray matter (GM), white matter (WM), and cerebrospinal fluid (CSF) (Zijdenbos et al., 1996). The hemispheric GM and WM surfaces were extracted using the Constrained Laplacian-based Automated Segmentation with Proximities (CLASP) (June et al., 2005), (MacDonald et al., 2000). Finally, the cortical thickness was measured using the Euclidean distance between the corresponding vertices of the GM and WM surfaces (Lerch and Evans, 2005).

2.3 AD-related regions of interest selection and statistical analysis

From 68 regions of interest (ROIs) provided by the AAL (Automated Anatomical Labeling) atlas, we selected 17 AD-associated brain regions based on a reference study (Lerch et al., 2005). Mean cortical thickness in each ROI, after making adjustments for age, sex, education, intracranial volume (ICV), and scanner magnetic field strength, was compared across disease groups using ANCOVA. The False Discovery Rate (FDR) method was implemented to address the multiple-comparisons problem.

2.4 Genotyping and quality control

We downloaded genotype data from ADNI website (http://www.loni.ucla.edu/ADNI). Genotyping was performed using the Illumina Human610-QuadBeadhChip in ADNI-1 and the Illumina HumanOmniExpress BeadChip in ADNI-GO/2 (Saykin et al., 2010), (Saykin et al., 2015). Un-genotyped SNPs from the ADNI-1 and ADNI-GO/2 GWAS data were imputed

separately using IMPUTE2 (Marchini et al., 2007) with the 1000 Genomes Project Phase 1 samples as a reference panel. We downloaded genotype data of two *APOE* SNPs (rs429358, and rs7412) that define ε2, ε3, and ε4 alleles from the ADNI website. The quality-control procedures were performed using PLINK v1.9 software (Purcell et al., 2007), where the individual markers that did not satisfy the following criteria were removed from the analysis: genotype call rate < 95%, Hardy-Weinberg equilibrium $p < 10^{-6}$ (in controls), and minor allele frequency (MAF) < 5%. Finally, 3,041,429 bi-allelic SNPs in autosomal chromosomes (that is, sex chromosomes, mitochondrial, and pseudo-autosomal SNPs were excluded) from subjects with European ancestry were used.

2.5 Genome-wide association study (GWAS)

The allelic effects for cortical thickness were measured using additive models considering age, sex, education, scanner field strength, *APOE* ε4 genotype, disease status, and ICV as covariates. Disease status is coded according to three variables (CN: 1, MCI: 2, and AD: 3), and *APOE* ε4 genotype represents the number of ε4 copies. As education levels are highly correlated with the cortical thickness (Jung et al., 2018; Seo et al., 2011), we used education as one of covariates and we used disease status as a covariate to reduce the possible environmental factors specific to AD patients such as treatment effects (Hass et al., 2013). APOE ε4 is a well-known genetic risk factor and highly correlated with disease status (Farlow, 2010), we used the APOE ε4 genotype as one of the covariates in order to identify APOE-independent genetic loci. To estimate the multiple testing burden associated with analyzing cortical thickness of 17 ROIs, we used permutation test (Dudbridge and Gusnanto, 2008), which yielded 13 independent phenotypes, and a multiple testing significance threshold of $p < 4.17 \times 10^{-9}$. We performed whole brain surface-based analysis for significant SNPs from GWAS using data from 919 GWA discovery samples and 629 replication samples.

Demographics and genotypic characteristics of the replication samples are described in Supplementary Table 1. The surface-based analysis of cortical thickness on a vertex-by-vertex was performed with the SurfStat MATLAB toolbox (http://www.math.mcgill.ca/keith/surfstat).

2.6 Association analysis with the severity of AD progression

Cortical thickness is an AD-related imaging biomarker and can be used to track disease progression (Pini et al., 2016). Furthermore, cortical thinning in AD-associated brain regions is known to be related to memory and cognitive declines that are the prominent symptoms of AD (Busovaca et al., 2016; Meiberth et al., 2015; Schultz et al., 2015). We hypothesized that the identified cortical thickness associated variants are associated with the severity of AD symptoms. We tested associations between two identified independent SNPs in two loci (rs661526, rs10109716) from GWAS and CDR scores (Clinical Dementia Rating) using linear regression after applying inverse normal transformation for data normality. Bonferroni corrected p-value < 0.05 was considered significant.

2.7 Expression quantitative trait locus (eQTL) analysis

We conducted an expression quantitative trait locus (eQTL) analysis to identify the functional effect of genetic variants on gene expression. To identify eQTLs, we leveraged the two most significant SNPs (rs661526, rs10109716) with the corresponding gene expression levels from the Braineac database (http://www.braineac.org/) (Ramasamy et al., 2014). Exon-specific expression levels in 10 brain tissues, including the hippocampus, cingulate, white matter, frontal, and occipital cortex were downloaded from the Braineac database, and eQTLs with an FDR-corrected p-value < 0.05 were considered significant.

2.8 Differential expression analysis

We tested differential expression of the identified genes between dementia and control subjects based on the normalized gene level (FPKM (Fragments Per Kilobase of transcripts per Million mapped reads) values) in the public database (http://aging.brain-map.org/). The gene expression levels of ST18 and NFIA in the hippocampus, parietal cortex, and temporal cortex were downloaded from the Aging, Dementia, and TBI Study (Allen et al., 2016). We tested the differential expressions of the genes in each brain region between age- and sex-matched dementia and control subjects. The differential expression analysis was performed using t-test and the significance level of FDR-corrected p-value < 0.05 was used.

2.9 Cell-type specific brain expression

We searched expression levels of the identified genes in mouse and human brain cells from the Brain RNA-Seq database (http://www.brainrnaseq.org/). This database provided gene expression levels across the brain cells, including neurons, oligodendrocytes, astrocytes, and microglia from the mouse (Zhang et al., 2014) and human brains (Zhang et al., 2016).

2.10 Pathway analysis

We conducted pathway analysis using GSA-SNP (Nam et al., 2010) to identify functional gene sets exhibiting the enrichment of associations in GWAS. The pathway annotations from the Gene Ontology (GO) resource were downloaded from the Molecular Signatures Database (http://software.broadinstitute.org/gsea/msigdb/), version 6.2. We compiled a list of 5,126 gene sets containing 5-200 genes in each pathway for this analysis to limit the potential for possible size-influenced association (Ramanan et al., 2015). SNPs that fell within 20 kb of the boundary of a gene were annotated to the corresponding gene on the human genome (hg19) coordinate.

A p-value of each SNP from GWAS summary statistics was used to estimate the gene score, and to avoid spurious predictions, the SNP with the second highest -log(SNP p-value) was used to summarize the association with each gene. Each pathway gene-set was assessed by Z-statistics for the identification of the enriched pathways, and pathways with FDR corrected p-value < 0.05 were considered significant.

3. Results

3.1 Mean cortical thickness in 17 AD-related ROIs

Mean cortical thicknesses and standard deviations of 17 ROIs (regions of interest) in three disease groups (AD, MCI, and CN) are summarized in Table 2. The statistical results of the differences in cortical thickness between the three groups are summarized in Table 2; the p-value was corrected using the FDR method. Most of the regions except for the right anterior cingulate and paracingulate gyri showed significant differences (FDR-corrected p-value < 0.05) between the three disease groups.

3.2 GWAS of mean cortical thickness

To identify susceptible genes of cortical thickness, we performed GWAS on mean cortical thicknesses of 17 AD-associated brain regions. All phenotypes were almost normally distributed across the full sample (Supplementary Fig. 1). No evidence of systematic bias was observed in the association results (Supplementary Fig. 2). The genome-wide significant associations were identified in two ROIs, the left inferior frontal gyrus (orbital part), and left parahippocampal gyrus (Fig. 1). For the left inferior frontal gyrus, 14 SNPs exceeded the genome-wide significance threshold (i.e., p-value $< 4.17 \times 10^{-9}$). An intronic SNP in *ST18* (ST18 C2H2C-type zinc finger transcription factor), rs10109716 on chromosome 8, showed the strongest association (p-value = 2.68×10^{-10}) (Fig. 2A). The concordance of SNPs within

the *ST18* gene between imputed data and whole-genome sequencing data was very high (99.89%). For the left parahippocampal gyrus, rs661526, one SNP near the *NFIA* (nuclear factor I A) on chromosome 1, showed the genome-wide significant association (p-value = 3.30×10^{-9}) (Fig. 2B). We performed whole brain surface-based analysis of cortical thickness on a vertex-by-vertex basis on the brain surface to examine the effects of two significant SNPs (rs10109716, rs661526) on brain structural changes across all cortical regions in the whole brain. The most significant SNP (rs661526) in *ST18* was associated with increased cortical thickness in the bilateral temporal lobes including the parahippocampal gyrus (within red circle), even after the adjustment for multiple comparisons using the random field theory (Supplementary Figure 3 (A)). The most significant SNP (rs10109716) in *NFIA* was associated with increased cortical thickness in a widespread pattern including the bilateral frontal, parietal, and temporal lobes, particularly in the inferior frontal gyrus (within red circle), even after the adjustment for multiple comparisons using the random field theory (Supplementary Figure 3 (C)). In order to replicate the findings of the two significant SNPs (rs10109716, rs661526) from whole brain analysis of cortical thickness, we used an independent data (N=629) from the ADNI cohort. In the replication study, the most significant SNP (rs661526) in *ST18* was associated with increased cortical thickness in the left parahippocampal gyrus (within red circle), which showed consistent patterns in the discovery study (Supplementary Figure 3 (B)). The most significant SNP (rs10109716) in *NFIA* was associated with increased cortical thickness in the left inferior frontal gyrus (within red circle), even after the adjustment for multiple comparisons using the random field theory, which showed same association directions in the discovery study (Supplementary Figure 3 (D)).

3.3 Association analysis of GWAS-identified SNPs with the severity of AD

We performed association analysis of two identified independent SNPs (rs661526, rs10109716) in two loci with CDR scores using linear regression. The rs10109716 in *ST18* on chromosome 8 showed statistically significant associations after Bonferroni correction (corrected p-value = 0.023) and rs661526 in *NFIA* did not show significant association with CDR scores (corrected p-value = 0.567).

3.4 Expression quantitative trait loci (eQTL)

To identify the functional effect of genetic variants on gene expression, we performed eQTL analysis. The SNPs identified from GWAS on chromosomes 1 and 8 have strong linkage disequilibrium (LD) with the two most significant SNPs (rs661526 and rs10109716). Our results showed that rs661526 on chromosome 1 significantly regulates expression levels of *NFIA* in the substantia nigra (FDR-corrected p-value = 2.90 x 10^{-2}) and frontal cortex (FDR-corrected p-value = 2.90 x 10^{-2}). Expression levels of *ST18* in the thalamus (FDR-corrected p-value = 3.90 x 10^{-2}) are regulated by rs10109716 on chromosome 8 (Fig. 3)

3.5 Differential expression analysis

For the two identified cortical thickness associated genes, we performed a t-test to compare gene expression levels in the hippocampus, parietal cortex, and temporal cortex between dementia and control subjects. We found that *NFIA* (p-value = 0.027, $\log_2$FC=0.093) was differentially expressed in the right hippocampus and *ST18* (p-value = 0.026, $\log_2$FC=0.32) in the right temporal cortex (Table 3).

3.6 Cell-type specific brain expression

We examined the expression patterns of two identified genes, ST18 and NFIA, across seven cells in the mouse (Supplementary Fig. 4) and 6 cells in the human brain (Supplementary Fig.

5). *ST18* was expressed at a higher level in newly formed oligodendrocyte (mean FPKM = 9.5) and oligodendrocyte (mean FPKM = 20) in the mouse and human brains, respectively. Moreover, *NFIA* was expressed at a higher level in astrocyte in both the mouse (mean FPKM = 19.3) and human brains (mean FPKM = 41.9).

3.7 Pathway analysis

To identify functional gene sets involved in cortical thickness atrophy, all SNP p-values from GWAS were used. We identified 46 gene sets displaying the enrichment of GWAS associations for the left inferior frontal gyrus (orbital part) and 22 gene sets for the left parahippocampal gyrus. The enriched GO terms included several pathways related to ion activity and cell organization and differentiation. More detailed results are presented in Supplementary Tables 2 and 3.

4. Discussion

We used mean cortical thicknesses of 17 AD-related ROIs as endophenotypes. Cortical thicknesses of these regions are significantly different between AD and CN (cognitive normal) subjects. Although statistical results in the right anterior cingulate and paracingulate gyri were slightly different than those reported in a previous study (Lerch et al., 2005), cortical thicknesses of these regions are also thinner in AD than in CN. The association between the selected ROIs and AD were reproducibly identified even in a different dataset. Our finding supports that cortical thickness of these regions is a valuable endophenotype for AD.

A total of 15 SNPs (single nucleotide polymorphism) exceeded the genome-wide significant p-value (p-value < 4.17 x 10^{-9}). A total of 14 of the identified SNPs are located in the genome regions of *ST18* (ST18 C2H2C-type zinc finger transcription factor) on chromosome 8, and the other one SNP is located near *NFIA* (nuclear factor I A) on chromosome 1.

ST18 is a protein-coding gene related to DNA-binding transcription factor activity. The gene has previously been linked to breast cancer, chronotype measurements, and dementia (Jandrig et al., 2004; Jansen et al., 2019; Pottier et al., 2018; Sherva et al., 2014). For example, *ST18* has been reported to be associated with cognitive decline in AD (Sherva et al., 2014). We showed that *ST18* was associated with CDR (Clinical Dementia Rating) scores that are characterized by a decline in cognitive and functional performance including memory performance. Our result indicates that *ST18* was associated with cognitive decline in AD.

ST18 is a transcription factor that regulates neuronal differentiation and plays an important role within a myelination network as a hub gene in late-onset AD (Humphries et al., 2015). Transcriptional changes in the myelination network were observed in AD (Miller et al., 2008), (Zhang et al., 2013) and demyelination is known as one of the important components of AD, along with Aβ plaques and neurofibrillary tangles (Sachdev et al., 2013), (Caso et al., 2016). Myelination results in saltatory conduction of action potentials that prominently increases the signal-transmission speed (Waxman, 1977), which makes it possible to integrate the information across highly distributed neural networks that underlie higher cognitive functions (Bartzokis, 2004; Fuster, 1999). Demyelination interrupts the synchronization of neuronal impulses and eventually destroys functional connections of cortical regions with subsequent neuronal dysfunction and degradation (Bartzokis, 2004). Functional disconnections of cortico-cortical communication, which primarily affect cognitive functions, are observed in the preclinical and early stages of AD (Bartzokis, 2004, 2002; BRAAK et al., 2006; Fox et al., 1998). Later myelinating brain regions such as inferior temporal and prefrontal regions that are proposed to be those most susceptible to neurodegeneration in AD are the focus of the very first deposition of Aβ and may be more susceptible to myelin breakdown than early-myelinating regions (BRAAK et al., 2006; Mitew et al., 2010; Thal et al., 2002). Thus, the

genetic effects that affect myelin development and breakdown will manifest as risk factors for AD.

ST18 is highly expressed in oligodendrocytes, which play an important role in myelin formation (Dong et al., 2018). Oligodendrocytes are associated with the production of cholesterol and cholesterol deficits in gray matter (GM), and they can directly influence synaptogenesis and dendritic outgrowth (Bartzokis, 2004; Fan et al., 2002; Mauch et al., 2001). Furthermore, iron contents in oligodendrocytes are associated with the production of amyloid precursor protein (APP), and iron and other metals make Aβ toxic, which is considered the primary pathogenic trigger of AD (Rogers et al., 2002), (Curtain et al., 2001). Oligodendrocyte precursor from later myelinating regions has a reduced myelin turnover, and thus, a diminished capacity for myelin repair (Mitew et al., 2010), (Power et al., 2002). In addition, rs10109716 is associated with expression levels of *ST18* in the thalamus. The thalamus plays a significant role in episodic memory, and therefore, it can impact the symptomology of AD (Acosta-Cabronero and Nestor, 2014; Aggleton et al., 2016; Harding, 2000; Van Der Werf et al., 2003). One out of the 15 GWAS-identified SNPs is located in the genomic region near *NFIA-AS2*, which encodes long non-coding RNA (Inc-RNA). Antisense lnc-RNAs are described from either the same genomic site or a site distant from the gene locus where the sense transcript counterpart is produced and either represses or activates transcription of the targeted protein-coding gene (Ling et al., 2013). Therefore, *NFIA-AS2* may be involved in the regulation of the expression of *NFIA* (Ahmetov et al., 2015). We suggest that rs661526, which is the most prominent SNP on chromosome 1, may be associated with the regulation of *NFIA*. Indeed, in our study, we have shown that rs661526 is associated with expression levels of *NFIA* in several brain regions including the frontal cortex and substantia nigra.

NFIA, a protein-coding gene, has previously been associated with bipolar disorder (Lee et al., 2013), a disease that is known to share common clinical, epigenetics, and molecular pathological mechanisms with AD (Corrêa-Velloso et al., 2018). *NFIA* has been reported to be upregulated in AD compared with control subjects and showed different expression levels depending on the different courses of AD. Briefly, this gene is upregulated in incipient and moderate AD but downregulated in severe AD (Kong et al., 2017). Furthermore, *NFIA* plays an important role in normal cortical development (Bunt et al., 2017). Mutations in NFIA have been reported to affect brain phenotypes, including agenesis of the corpus callosum, the disruption of midline fusion, enlargement of ventricles, and malformation of the hippocampus (Gobius et al., 2016; Koehler et al., 2010; Lu et al., 2007), where the deformations of these brain phenotypes are significantly associated with AD (Dickerson et al., 2001; Nestor et al., 2008; Teipel et al., 2002).

NFIA is highly expressed in astrocytes in the brains of both humans and mice. *NFIA* plays a crucial role at the initial stage of astrocytes differentiation (Wilczynska et al., 2009). Astrocytes are critical to both brain functioning and development; they provide overall brain homeostasis, assist in neurogenesis, and determine the micro-architecture of the grey matter (Verkhratsky et al., 2010). Furthermore, astrocytes are specifically involved in the progression of neuropathological states, including neuroinflammation associated with neurodegenerative diseases such as AD (Wilczynska et al., 2009). These findings highlight the importance of *NFIA* in the cortical structure. However, the relationship between *NFIA* and the left parahippocampal gyrus must be tested in future studies.

We performed pathway-based analysis and identified 68 pathways including ion-channel activity and cell differentiation and organization. Ion channels, including sodium, potassium, and calcium channels, are implicated in neurodegenerative diseases. For instance, potassium channels have been implicated in the onset of long-term potentiation in mammalian neurons,

which is thought to underlie learning and memory (Kidd et al., 2006). Altered calcium signaling accelerates Aβ formation, which is the hallmark of AD, and Aβ disrupts the calcium homeostasis that induces apoptosis in neurons (Ekinci et al., 2000), (Abramov et al., 2004). This cycle of Aβ generation and calcium perturbation leads to synaptic breakdown, cell death, and devastating memory loss (Demuro et al., 2010). AD is caused by not only the accumulation of Aβ and tau but also the effects of dysfunction and loss of synapses (Forner et al., 2017). Synapse assembly determines the functional outputs of the nervous system which deterioration is the characteristic of AD, including learning, memory, and cognition (Batool et al., 2019; Taoufik et al., 2018). Furthermore, Aβ and tau have been reported to cause synaptic dysfunctions, thereby giving rise to neurodegenerative disorders including AD (Forner et al., 2017).

This study has several limitations. Although we used T1-weighted images and genetic data from the publicly available ADNI datasets, our sample size is moderate for a genetic association study. Our GWAS showed regionally heterogeneous results, and we could not elucidate the direct effect of genetic loci on AD-related brain regions. We performed functional analyses of identified SNPs and association analysis with the severity score of AD, but our sample size is moderate and we did not use a replication dataset. Thus, the replication of our findings in independent larger datasets is required.

In conclusion, we performed GWAS of mean cortical thicknesses of 17 AD-related ROIs to identify novel associations in *ST18* and *NFIA* with mean cortical thicknesses in the left inferior frontal gyrus and left parahippocampal gyrus, respectively. These genes were also associated with CDR scores. The functional roles of these genes could provide new insights into the brain structural atrophy, particularly in AD.

Acknowledgements

ADNI data are disseminated by the Laboratory for Neuro Imaging at the University of Southern California.

Author contribution

Bo-Hyun Kim: Conceptualization, Methodology, Writing- Original draft preparation.

Kwangsik Nho: Data curation, Investigation, Writing- Reviewing and Editing.

Jong-Min Lee: Conceptualization, Supervision, Writing- Reviewing and Editing**.**

Verification

We verify that the work described has not been published previously, that it is not under consideration for publication elsewhere, that its publication is approved by all authors and tacitly or explicitly by the responsible authorities where the work was carried out, and that, if accepted, it will not be published elsewhere in the same form, in English or in any other language, including electronically without the written consent of the copyright-holder.

References

Abramov, A.Y., Canevari, L., Duchen, M.R., 2004. Calcium signals induced by amyloid β peptide and their consequences in neurons and astrocytes in culture, in: Biochimica et Biophysica Acta - Molecular Cell Research. pp. 81–87. https://doi.org/10.1016/j.bbamcr.2004.09.006

Acosta-Cabronero, J., Nestor, P.J., 2014. Diffusion tensor imaging in Alzheimer's disease: Insights into the limbic-diencephalic network and methodological considerations. Front. Aging Neurosci. 6. https://doi.org/10.3389/fnagi.2014.00266

Aggleton, J.P., Pralus, A., Nelson, A.J.D., Hornberger, M., 2016. Thalamic pathology and memory loss in early Alzheimer's disease: Moving the focus from the medial temporal lobe to Papez circuit. Brain. https://doi.org/10.1093/brain/aww083

Ahmetov, I.I., Kulemin, N.A., Popov, D. V., Naumov, V.A., Akimov, E.B., Bravy, Y.R., Egorova, E.S., Galeeva, A.A., Generozov, E. V., Kostryukova, E.S., Larin, A.K., Mustafina, L.J., Ospanova, E.A., Pavlenko, A. V., Starnes, L.M., Zmijewski, P., Alexeev, D.G., Vinogradova, O.L., Govorun, V.M., 2015. Genome-wide association study identifies three novel genetic markers associated with elite endurance performance. Biol. Sport 32, 3–9. https://doi.org/10.5604/20831862.1124568

Allen, M., Carrasquillo, M.M., Funk, C., Heavner, B.D., Zou, F., Younkin, C.S., Burgess, J.D., Chai, H.S., Crook, J., Eddy, J.A., Li, H., Logsdon, B., Peters, M.A., Dang, K.K., Wang, X., Serie, D., Wang, C., Nguyen, T., Lincoln, S., Malphrus, K., Bisceglio, G., Li, M., Golde, T.E., Mangravite, L.M., Asmann, Y., Price, N.D., Petersen, R.C., Graff-Radford, N.R., Dickson, D.W., Younkin, S.G., Ertekin-Taner, N., 2016. Human whole genome genotype and transcriptome data for Alzheimer's and other neurodegenerative diseases. Sci. Data 3. https://doi.org/10.1038/sdata.2016.89

Bartzokis, G., 2004. Age-related myelin breakdown: a developmental model of cognitive decline and Alzheimer's disease. Neurobiol. Aging 25, 5–18; author reply 49-62. https://doi.org/10.1016/j.neurobiolaging.2003.03.001

Bartzokis, G., 2002. Schizophrenia: Breakdown in the well-regulated lifelong process of brain development and maturation. Neuropsychopharmacology 27, 672–683. https://doi.org/10.1016/S0893-133X(02)00364-0

Batool, S., Raza, H., Zaidi, J., Riaz, S., Hasan, S., Syed, N.I., 2019. Synapse formation: From cellular and molecular mechanisms to neurodevelopmental and neurodegenerative disorders. J. Neurophysiol. 121, 1381–1397. https://doi.org/10.1152/jn.00833.2018

Bettens, K., Sleegers, K., Van Broeckhoven, C., 2013. Genetic insights in Alzheimer's disease. Lancet Neurol. https://doi.org/10.1016/S1474-4422(12)70259-4

Blanco-Gómez, A., Castillo-Lluva, S., del Mar Sáez-Freire, M., Hontecillas-Prieto, L., Mao, J.H., Castellanos-Martín, A., Pérez-Losada, J., 2016. Missing heritability of complex diseases: Enlightenment by genetic variants from intermediate phenotypes. BioEssays 38, 664–673. https://doi.org/10.1002/bies.201600084

BRAAK, H., TREDICI, K., SCHULTZ, C., BRAAK, E., 2006. Vulnerability of Select Neuronal Types to Alzheimer's Disease. Ann. N. Y. Acad. Sci. 924, 53–61. https://doi.org/10.1111/j.1749-6632.2000.tb05560.x

Braskie, M.N., Ringman, J.M., Thompson, P.M., 2011. Neuroimaging measures as endophenotypes in Alzheimer's disease. Int. J. Alzheimers. Dis. https://doi.org/10.4061/2011/490140

Bunt, J., Osinski, J.M., Lim, J.W., Vidovic, D., Ye, Y., Zalucki, O., O'Connor, T.R., Harris, L., Gronostajski, R.M., Richards, L.J., Piper, M., 2017. Combined allelic dosage of Nfia and Nfib regulates cortical development . Brain Neurosci. Adv. 1, 239821281773943. https://doi.org/10.1177/2398212817739433

Caso, F., Agosta, F., Filippi, M., 2016. Insights into white matter damage in Alzheimer's disease: From postmortem to in vivo diffusion tensor MRI studies, in: Neurodegenerative Diseases. pp. 26–33. https://doi.org/10.1159/000441422

Collins, D.L., Neelin, P., Peters, T.M., Evans, A.C., 1994. Automatic 3d intersubject registration of mr volumetric data in standardized talairach space. J. Comput. Assist. Tomogr. 18, 192–205. https://doi.org/10.1097/00004728-199403000-00005

Consortium, T.Gte., Ardlie, K.G., Deluca, D.S., Segrè, A. V., Sullivan, T.J., Young, T.R., Gelfand, E.T., Trowbridge, C.A., Maller, J.B., Tukiainen, T., Lek, M., Ward, L.D., Kheradpour, P., Iriarte, B., Meng, Y., Palmer, C.D., Esko, T., Winckler, W., Hirschhorn, J.N., Kellis, M., MacArthur, D.G., Getz, G., Shabalin, A.A., Li, G., Zhou, Y.-H., Nobel, A.B., Rusyn, I., Wright, F.A., Lappalainen, T., Ferreira, P.G., Ongen, H., Rivas, M.A., Battle, A., Mostafavi, S., Monlong, J., Sammeth, M., Mele, M., Reverter, F., Goldmann, J.M., Koller, D., Guigó, R., McCarthy, M.I., Dermitzakis, E.T., Gamazon, E.R., Im, H.K., Konkashbaev, A., Nicolae, D.L., Cox, N.J., Flutre, T., Wen, X., Stephens, M., Pritchard, J.K., Tu, Z., Zhang, B., Huang, T., Long, Q., Lin, L., Yang, J., Zhu, J., Liu, J., Brown, A., Mestichelli, B., Tidwell, D., Lo, E., Salvatore, M., Shad, S., Thomas, J.A., Lonsdale, J.T., Moser, M.T., Gillard, B.M., Karasik, E., Ramsey, K., Choi, C., Foster, B.A., Syron, J., Fleming, J., Magazine, H., Hasz, R., Walters, G.D., Bridge, J.P., Miklos, M., Sullivan, S., Barker, L.K., Traino, H.M., Mosavel, M., Siminoff, L.A., Valley, D.R., Rohrer, D.C., Jewell, S.D., Branton, P.A., Sobin, L.H., Barcus, M., Qi, L., McLean, J., Hariharan, P., Um, K.S., Wu, S., Tabor, D., Shive, C., Smith, A.M., Buia, S.A., Undale, A.H., Robinson, K.L., Roche, N., Valentino, K.M., Britton, A., Burges, R., Bradbury, D., Hambright, K.W., Seleski, J., Korzeniewski, G.E., Erickson, K., Marcus, Y., Tejada, J., Taherian, M., Lu, C., Basile, M., Mash, D.C., Volpi, S., Struewing, J.P., Temple, G.F., Boyer, J., Colantuoni, D., Little, R., Koester, S., Carithers, L.J., Moore, H.M., Guan, P.,

Compton, C., Sawyer, S.J., Demchok, J.P., Vaught, J.B., Rabiner, C.A., Lockhart, N.C., Ardlie, K.G., Getz, G., Wright, F.A., Kellis, M., Volpi, S., Dermitzakis, E.T., 2015. The Genotype-Tissue Expression (GTEx) pilot analysis: Multitissue gene regulation in humans. Science (80-.). 348, 648–660. https://doi.org/10.1126/science.1262110

Corrêa-Velloso, J.C., Gonçalves, M.C., Naaldijk, Y., Oliveira-Giacomelli, Á., Pillat, M.M., Ulrich, H., 2018. Pathophysiology in the comorbidity of Bipolar Disorder and Alzheimer's Disease: pharmacological and stem cell approaches. Prog. Neuro-Psychopharmacology Biol. Psychiatry. https://doi.org/10.1016/j.pnpbp.2017.04.033

Curtain, C.C., Ali, F., Volitakis, I., Cherny, R.A., Norton, R.S., Beyreuther, K., Barrow, C.J., Masters, C.L., Bush, A.I., Barnham, K.J., 2001. Alzheimer's disease amyloid-{beta} binds Cu and Zn to generate an allosterically-ordered membrane-penetrating structure containing SOD-like subunits. J.Biol.Chem.

Demuro, A., Parker, I., Stutzmann, G.E., 2010. Calcium signaling and amyloid toxicity in Alzheimer disease. J. Biol. Chem. https://doi.org/10.1074/jbc.R109.080895

Dickerson, B.C., Bakkour, A., Salat, D.H., Feczko, E., Pacheco, J., Greve, D.N., Grodstein, F., Wright, C.I., Blacker, D., Rosas, H.D., Sperling, R.A., Atri, A., Growdon, J.H., Hyman, B.T., Morris, J.C., Fischl, B., Buckner, R.L., 2009. The cortical signature of Alzheimer's disease: Regionally specific cortical thinning relates to symptom severity in very mild to mild AD dementia and is detectable in asymptomatic amyloid-positive individuals. Cereb. Cortex 19, 497–510. https://doi.org/10.1093/cercor/bhn113

Dickerson, B.C., Goncharova, I., Sullivan, M.P., Forchetti, C., Wilson, R.S., Bennett, D.A., Beckett, L.A., DeToledo-Morrell, L., 2001. MRI-derived entorhinal and hippocampal atrophy in incipient and very mild Alzheimer's disease. Neurobiol. Aging 22, 747–754. https://doi.org/10.1016/S0197-4580(01)00271-8

Dong, Y.X., Zhang, H.Y., Li, H.Y., Liu, P.H., Sui, Y., Sun, X.H., 2018. Association between Alzheimer's disease pathogenesis and early demyelination and oligodendrocyte dysfunction. Neural Regen. Res. 13, 908–914. https://doi.org/10.4103/1673-5374.232486

Doraiswamy, P.M., Sperling, R.A., Johnson, K., Reiman, E.M., Wong, T.Z., Sabbagh, M.N., Sadowsky, C.H., Fleisher, A.S., Carpenter, A., Joshi, A.D., Lu, M., Grundman, M., Mintun, M.A., Skovronsky, D.M., Pontecorvo, M.J., Duara, R., Sabbagh, M., Ahern, G.L., Holub, R.F., Farmer, M. V., Safirstein, B.E., Alva, G., Longmire, C.F., Jewell, G., Johnson, K.A., Korn, R., Wendt, J.K., Wong, D., Coleman, R.E., Devous, M., Jennings, D., Weiner, M.W., Murphy, C.A., Kovnat, K.D., Williamson, J.D., 2014. Florbetapir F 18 amyloid PET and 36-month cognitive decline:a prospective multicenter study. Mol. Psychiatry 19, 1044–1051. https://doi.org/10.1038/mp.2014.9

Du, A.-T., Schuff, N., Kramer, J.H., Rosen, H.J., Gorno-Tempini, M.L., Rankin, K., Miller, B.L., Weiner, M.W., 2007. Different regional patterns of cortical thinning in Alzheimer's disease and frontotemporal dementia. Brain 130, 1159–66. https://doi.org/10.1093/brain/awm016

Dudbridge, F., Gusnanto, A., 2008. Estimation of significance thresholds for genomewide association scans. Genet. Epidemiol. https://doi.org/10.1002/gepi.20297

E., W., A.J., L., B., S., L., G., I., R., 2007. APOE status and its association to learning and memory performance in middle aged and older Norwegians seeking assessment for memory deficits. Behav. Brain Funct. 3. https://doi.org/10.1186/1744-9081-3-57 LK - http://sfx.library.uu.nl/utrecht?sid=EMBASE&issn=17449081&id=doi:10.1186%2F174 4-9081-3-57&atitle=APOE+status+and+its+association+to+learning+and+memory+performance +in+middle+aged+and+older+Norwegians+seeking+assessment+for+memory+deficits

&stitle=Behav.+Brain+Funct.&title=Behavioral+and+Brain+Functions&volume=3&iss

ue=&spage=&epage=&aulast=Wehling&aufirst=Eike&auinit=E.&aufull=Wehling+E.&

coden=&isbn=&pages=-&date=2007&auinit1=E&auinitm=

Ekinci, F.J., Linsley, M.D., Shea, T.B., 2000. β-Amyloid-induced calcium influx induces

apoptosis in culture by oxidative stress rather than tau phosphorylation. Mol. Brain Res.

76, 389–395. https://doi.org/10.1016/S0169-328X(00)00025-5

Fan, Q.W., Yu, W., Gong, J.S., Zou, K., Sawamura, N., Senda, T., Yanagisawa, K.,

Michikawa, M., 2002. Cholesterol-dependent modulation of dendrite outgrowth and

microtubule stability in cultured neurons. J. Neurochem. 80, 178–190.

https://doi.org/10.1046/j.0022-3042.2001.00686.x

Farlow, M.R., 2010. Should the ApoE genotype be a covariate for clinical trials in Alzheimer

disease? Alzheimer's Res. Ther. https://doi.org/10.1186/alzrt39

Forner, S., Baglietto-Vargas, D., Martini, A.C., Trujillo-Estrada, L., LaFerla, F.M., 2017.

Synaptic Impairment in Alzheimer's Disease: A Dysregulated Symphony. Trends

Neurosci. https://doi.org/10.1016/j.tins.2017.04.002

Fox, N., Warrington, E.K., Seiffer, A.L., Agnew, S.K., Rossor, M.N., 1998. Presymptomatic

cognitive deficits in individuals at risk of familial Alzheimer's disease. Brain 121,

1631–1639.

Fuster, J.M., 1999. Synopsis of function and dysfunction of the frontal lobe, in: Acta

Psychiatrica Scandinavica, Supplement. pp. 51–57. https://doi.org/10.1111/j.1600-

0447.1999.tb05983.x

Gobius, I., Morcom, L., Suárez, R., Bunt, J., Bukshpun, P., Reardon, W., Dobyns, W.B.,

Rubenstein, J.L.R., Barkovich, A.J., Sherr, E.H., Richards, L.J., 2016. Astroglial-

Mediated Remodeling of the Interhemispheric Midline Is Required for the Formation of

the Corpus Callosum. Cell Rep. 17, 735–747.

https://doi.org/10.1016/j.celrep.2016.09.033

Gomez-Isla, T., West, H.L., Rebeck, G.W., Harr, S.D., Growdon, J.H., Locascio, J.J., Perls,
T.T., Lipsitz, L.A., Hyman, B.T., 1996. Clinical and pathological correlates of
apolipoprotein ε4 in Alzheimer's disease. Ann. Neurol. 39, 62–70.
https://doi.org/10.1002/ana.410390110

Harding, A., 2000. Degeneration of anterior thalamic nuclei differentiates alcoholics with
amnesia. Brain 123, 141–154. https://doi.org/10.1093/brain/123.1.141

Hass, J., Walton, E., Kirsten, H., Liu, J., Priebe, L., Wolf, C., Karbalai, N., Gollub, R., White,
T., Roessner, V., Müller, K.U., Paus, T., Smolka, M.N., Schumann, G., Scholz, M.,
Cichon, S., Calhoun, V., Ehrlich, S., 2013. A Genome-Wide Association Study Suggests
Novel Loci Associated with a Schizophrenia-Related Brain-Based Phenotype. PLoS
One. https://doi.org/10.1371/journal.pone.0064872

Hirschhorn, J.N., Daly, M.J., 2005. Genome-wide association studies for common diseases
and complex traits. Nat. Rev. Genet. https://doi.org/10.1038/nrg1521

Humphries, C.E., Kohli, M.A., Nathanson, L., Whitehead, P., Beecham, G., Martin, E., Mash,
D.C., Pericak-Vance, M.A., Gilbert, J., 2015. Integrated whole transcriptome and DNA
methylation analysis identifies gene networks specific to late-onset Alzheimer's disease.
J. Alzheimer's Dis. 44, 977–987. https://doi.org/10.3233/JAD-141989

Jack, C.R., Bernstein, M.A., Fox, N.C., Thompson, P., Alexander, G., Harvey, D., Borowski,
B., Britson, P.J., Whitwell, J.L., Ward, C., Dale, A.M., Felmlee, J.P., Gunter, J.L., Hill,
D.L.G., Killiany, R., Schuff, N., Fox-Bosetti, S., Lin, C., Studholme, C., DeCarli, C.S.,
Krueger, G., Ward, H.A., Metzger, G.J., Scott, K.T., Mallozzi, R., Blezek, D., Levy, J.,
Debbins, J.P., Fleisher, A.S., Albert, M., Green, R., Bartzokis, G., Glover, G., Mugler, J.,

Weiner, M.W., 2008a. The Alzheimer's Disease Neuroimaging Initiative (ADNI): MRI

methods. J. Magn. Reson. Imaging 27, 685–691. https://doi.org/10.1002/jmri.21049

Jack, C.R., Bernstein, M.A., Fox, N.C., Thompson, P., Alexander, G., Harvey, D., Borowski,

B., Britson, P.J., Whitwell, J.L., Ward, C., Dale, A.M., Felmlee, J.P., Gunter, J.L., Hill,

D.L.G., Killiany, R., Schuff, N., Fox-Bosetti, S., Lin, C., Studholme, C., DeCarli, C.S.,

Krueger, G., Ward, H.A., Metzger, G.J., Scott, K.T., Mallozzi, R., Blezek, D., Levy, J.,

Debbins, J.P., Fleisher, A.S., Albert, M., Green, R., Bartzokis, G., Glover, G., Mugler, J.,

Weiner, M.W., 2008b. The Alzheimer's Disease Neuroimaging Initiative (ADNI): MRI

methods. J. Magn. Reson. Imaging. https://doi.org/10.1002/jmri.21049

Jandrig, B., Seitz, S., Hinzmann, B., Arnold, W., Micheel, B., Koelble, K., Siebert, R.,

Schwartz, A., Ruecker, K., Schlag, P.M., Scherneck, S., Rosenthal, A., 2004. ST18 is a

breast cancer tumor suppressor gene at human chromosome 8q11.2. Oncogene 23,

9295–9302. https://doi.org/10.1038/sj.onc.1208131

Jansen, P.R., Watanabe, K., Stringer, S., Skene, N., Bryois, J., Hammerschlag, A.R., de

Leeuw, C.A., Benjamins, J.S., Muñoz-Manchado, A.B., Nagel, M., Savage, J.E.,

Tiemeier, H., White, T., Agee, M., Alipanahi, B., Auton, A., Bell, R.K., Bryc, K., Elson,

S.L., Fontanillas, P., Furlotte, N.A., Hinds, D.A., Huber, K.E., Kleinman, A., Litterman,

N.K., McCreight, J.C., McIntyre, M.H., Mountain, J.L., Noblin, E.S., Northover,

C.A.M., Pitts, S.J., Sathirapongsasuti, J.F., Sazonova, O. V., Shelton, J.F., Shringarpure,

S., Tian, C., Wilson, C.H., Tung, J.Y., Hinds, D.A., Vacic, V., Wang, X., Sullivan, P.F.,

van der Sluis, S., Polderman, T.J.C., Smit, A.B., Hjerling-Leffler, J., Van Someren,

E.J.W., Posthuma, D., 2019. Genome-wide analysis of insomnia in 1,331,010

individuals identifies new risk loci and functional pathways. Nat. Genet. 51, 394–403.

https://doi.org/10.1038/s41588-018-0333-3

Jun, G., 2010. Meta-analysis Confirms CR1, CLU, and PICALM as Alzheimer Disease Risk Loci and Reveals Interactions With APOE Genotypes. Arch. Neurol. 67, 1473. https://doi.org/10.1001/archneurol.2010.201

June, S.K., Singh, V., Jun, K.L., Lerch, J., Ad-Dab'bagh, Y., MacDonald, D., Jong, M.L., Kim, S.I., Evans, A.C., 2005. Automated 3-D extraction and evaluation of the inner and outer cortical surfaces using a Laplacian map and partial volume effect classification. Neuroimage 27, 210–221. https://doi.org/10.1016/j.neuroimage.2005.03.036

Jung, N.Y., Cho, H., Kim, Y.J., Kim, H.J., Lee, J.M., Park, S., Kim, S.T., Kim, E.J., Kim, J.S., Moon, S.H., Lee, J.H., Ewers, M., Na, D.L., Seo, S.W., 2018. The impact of education on cortical thickness in amyloid-negative subcortical vascular dementia: Cognitive reserve hypothesis. Alzheimer's Res. Ther. https://doi.org/10.1186/s13195-018-0432-5

Kale, V. V., Hamde, S.T., Holambe, R.S., 2019. Multi class disorder detection of magnetic resonance brain images using composite features and neural network. Biomed. Eng. Lett. 9, 221–231. https://doi.org/10.1007/s13534-019-00103-1

Karch, C.M., Cruchaga, C., Goate, A.M., 2014. Alzheimer's disease genetics: From the bench to the clinic. Neuron. https://doi.org/10.1016/j.neuron.2014.05.041

Kidd, J.F., Brown, L.A., Sattelle, D.B., 2006. Effects of amyloid peptides on A-type K+ currents of Drosophila larval cholinergic neurons. J. Neurobiol. 66, 476–487. https://doi.org/10.1002/neu.20227

Koehler, U., Holinski-Feder, E., Ertl-Wagner, B., Kunz, J., von Moers, A., von Voss, H., Schell-Apacik, C., 2010. A novel 1p31.3p32.2 deletion involving the NFIA gene detected by array CGH in a patient with macrocephaly and hypoplasia of the corpus callosum. Eur. J. Pediatr. 169, 463–468. https://doi.org/10.1007/s00431-009-1057-2

Kong, W., Mou, X., Deng, J., Di, B., Zhong, R., Wang, S., Yang, Y., Zeng, W., 2017.

Differences of immune disorders between Alzheimer's disease and breast cancer based

on transcriptional regulation. PLoS One 12.

https://doi.org/10.1371/journal.pone.0180337

Lambert, J.-C., Ibrahim-Verbaas, C.A., Harold, D., Naj, A.C., Sims, R., Bellenguez, C., Jun,

G., DeStefano, A.L., Bis, J.C., Beecham, G.W., Grenier-Boley, B., Russo, G., Thornton-

Wells, T.A., Jones, N., Smith, A. V, Chouraki, V., Thomas, C., Ikram, M.A., Zelenika,

D., Vardarajan, B.N., Kamatani, Y., Lin, C.-F., Gerrish, A., Schmidt, H., Kunkle, B.,

Dunstan, M.L., Ruiz, A., Bihoreau, M.-T., Choi, S.-H., Reitz, C., Pasquier, F.,

Hollingworth, P., Ramirez, A., Hanon, O., Fitzpatrick, A.L., Buxbaum, J.D., Campion,

D., Crane, P.K., Baldwin, C., Becker, T., Gudnason, V., Cruchaga, C., Craig, D., Amin,

N., Berr, C., Lopez, O.L., De Jager, P.L., Deramecourt, V., Johnston, J.A., Evans, D.,

Lovestone, S., Letenneur, L., Morón, F.J., Rubinsztein, D.C., Eiriksdottir, G., Sleegers,

K., Goate, A.M., Fiévet, N., Huentelman, M.J., Gill, M., Brown, K., Kamboh, M.I.,

Keller, L., Barberger-Gateau, P., McGuinness, B., Larson, E.B., Green, R., Myers, A.J.,

Dufouil, C., Todd, S., Wallon, D., Love, S., Rogaeva, E., Gallacher, J., St George-

Hyslop, P., Clarimon, J., Lleo, A., Bayer, A., Tsuang, D.W., Yu, L., Tsolaki, M., Bossù,

P., Spalletta, G., Proitsi, P., Collinge, J., Sorbi, S., Sanchez-Garcia, F., Fox, N.C., Hardy,

J., Naranjo, M.C.D., Bosco, P., Clarke, R., Brayne, C., Galimberti, D., Mancuso, M.,

Matthews, F., Moebus, S., Mecocci, P., Del Zompo, M., Maier, W., Hampel, H., Pilotto,

A., Bullido, M., Panza, F., Caffarra, P., Nacmias, B., Gilbert, J.R., Mayhaus, M.,

Lannfelt, L., Hakonarson, H., Pichler, S., Carrasquillo, M.M., Ingelsson, M., Beekly, D.,

Alvarez, V., Zou, F., Valladares, O., Younkin, S.G., Coto, E., Hamilton-Nelson, K.L.,

Gu, W., Razquin, C., Pastor, P., Mateo, I., Owen, M.J., Faber, K.M., Jonsson, P. V,

Combarros, O., O'Donovan, M.C., Cantwell, L.B., Soininen, H., Blacker, D., Mead, S.,

Mosley, T.H., Bennett, D.A., Harris, T.B., Fratiglioni, L., Holmes, C., de Bruijn, R.F.A.G., Passmore, P., Montine, T.J., Bettens, K., Rotter, J.I., Brice, A., Morgan, K., Foroud, T.M., Kukull, W.A., Hannequin, D., Powell, J.F., Nalls, M.A., Ritchie, K., Lunetta, K.L., Kauwe, J.S.K., Boerwinkle, E., Riemenschneider, M., Boada, M., Hiltunen, M., Martin, E.R., Schmidt, R., Rujescu, D., Wang, L.-S., Dartigues, J.-F., Mayeux, R., Tzourio, C., Hofman, A., Nöthen, M.M., Graff, C., Psaty, B.M., Jones, L., Haines, J.L., Holmans, P.A., Lathrop, M., Pericak-Vance, M.A., Launer, L.J., Farrer, L.A., van Duijn, C.M., Van Broeckhoven, C., Moskvina, V., Seshadri, S., Williams, J., Schellenberg, G.D., Amouyel, P., 2013. Meta-analysis of 74,046 individuals identifies 11 new susceptibility loci for Alzheimer's disease. Nat. Genet. 45, 1452–1458. https://doi.org/10.1038/ng.2802

Lee, H., Goo, H., Greenwood, T.A., Kripke, D.F., Kelsoe, J.R., 2013. A genome-wide association study of seasonal pattern mania identifies NF1A as a possible susceptibility gene for bipolar disorder. J. Affect. Disord. 145, 200–207. https://doi.org/10.1016/j.jad.2012.07.032

Lenzenweger, M.F., 2013a. ENDOPHENOTYPE, INTERMEDIATE PHENOTYPE, BIOMARKER: DEFINITIONS, CONCEPT COMPARISONS, CLARIFICATIONS. Depress. Anxiety 30, 185–189. https://doi.org/10.1002/da.22042

Lenzenweger, M.F., 2013b. Thinking clearly about the endophenotype-intermediate phenotype-biomarker distinctions in developmental psychopathology research. Dev. Psychopathol. 25, 1347–1357. https://doi.org/10.1017/S0954579413000655

Lerch, J.P., Evans, A.C., 2005. Cortical thickness analysis examined through power analysis and a population simulation. Neuroimage 24, 163–173. https://doi.org/10.1016/j.neuroimage.2004.07.045

Lerch, J.P., Pruessner, J.C., Zijdenbos, A., Hampel, H., Teipel, S.J., Evans, A.C., 2005. Focal decline of cortical thickness in Alzheimer's disease identified by computational neuroanatomy. Cereb. Cortex 15, 995–1001. https://doi.org/10.1093/cercor/bhh200

Ling, H., Fabbri, M., Calin, G.A., 2013. MicroRNAs and other non-coding RNAs as targets for anticancer drug development. Nat. Rev. Drug Discov. 12, 847–865. https://doi.org/10.1038/nrd4140

Lu, W., Quintero-Rivera, F., Fan, Y., Alkuraya, F.S., Donovan, D.J., Xi, Q., Turbe-Doan, A., Li, Q.G., Campbell, C.G., Shanske, A.L., Sherr, E.H., Ahmad, A., Peters, R., Rilliet, B., Parvex, P., Bassuk, A.G., Harris, D.J., Ferguson, H., Kelly, C., Walsh, C.A., Gronostajski, R.M., Devriendt, K., Higgins, A., Ligon, A.H., Quade, B.J., Morton, C.C., Gusella, J.F., Maas, R.L., 2007. NFIA haploinsufficiency is associated with a CNS malformation syndrome and urinary tract defects. PLoS Genet. 3, 830–843. https://doi.org/10.1371/journal.pgen.0030080

MacDonald, D., Kabani, N., Avis, D., Evans, A.C., 2000. Automated 3-D extraction of inner and outer surfaces of cerebral cortex from MRI. Neuroimage 12, 340–356. https://doi.org/10.1006/nimg.1999.0534

Manchia, M., Cullis, J., Turecki, G., Rouleau, G.A., Uher, R., Alda, M., 2013. The Impact of Phenotypic and Genetic Heterogeneity on Results of Genome Wide Association Studies of Complex Diseases. PLoS One 8, 1–7. https://doi.org/10.1371/journal.pone.0076295

Mauch, D.H., Nägier, K., Schumacher, S., Göritz, C., Müller, E.C., Otto, A., Pfrieger, F.W., 2001. CNS synaptogenesis promoted by glia-derived cholesterol. Science (80-.). 294, 1354–1357. https://doi.org/10.1126/science.294.5545.1354

Maxwell, T.J., Corcoran, C., Del-Aguila, J.L., Budde, J.P., Deming, Y., Cruchaga, C., Goate, A.M., Kauwe, J.S.K., 2018. Genome-wide association study for variants that modulate

relationships between cerebrospinal fluid amyloid-beta 42, tau, and p-tau levels. Alzheimer's Res. Ther. 10. https://doi.org/10.1186/s13195-018-0410-y

Meyer-Lindenberg, A., Weinberger, D.R., 2006. Intermediate phenotypes and genetic mechanisms of psychiatric disorders. Nat. Rev. Neurosci. 7, 818–827. https://doi.org/10.1038/nrn1993

Miller, J.A., Oldham, M.C., Geschwind, D.H., 2008. A Systems Level Analysis of Transcriptional Changes in Alzheimer's Disease and Normal Aging. J. Neurosci. 28, 1410–1420. https://doi.org/10.1523/JNEUROSCI.4098-07.2008

Mitew, S., Kirkcaldie, M.T.K., Halliday, G.M., Shepherd, C.E., Vickers, J.C., Dickson, T.C., 2010. Focal demyelination in Alzheimer's disease and transgenic mouse models. Acta Neuropathol. 119, 567–577. https://doi.org/10.1007/s00401-010-0657-2

Mueller, Susanne G., Weiner, M.W., Thal, L.J., Petersen, R.C., Jack, C., Jagust, W., Trojanowski, J.Q., Toga, A.W., Beckett, L., 2005. The Alzheimer's disease neuroimaging initiative. Neuroimaging Clin. N. Am. https://doi.org/10.1016/j.nic.2005.09.008

Mueller, Susanne G, Weiner, M.W., Thal, L.J., Petersen, R.C., Jack, C.R., Jagust, W., Trojanowski, J.Q., Toga, A.W., Beckett, L., 2005. Ways toward an early diagnosis in Alzheimer's disease: the Alzheimer's Disease Neuroimaging Initiative (ADNI). Alzheimers. Dement. 1, 55–66. https://doi.org/10.1016/j.jalz.2005.06.003

Murphy, G.M., Taylor, J., Kraemer, H.C., Yesavage, J., Tinklenberg, J.R., 1997. No association between Apolipoprotein E ε4 allele and rate of decline in Alzheimer's disease. Am. J. Psychiatry 154, 603–608. https://doi.org/10.1176/ajp.154.5.603

Nam, D., Kim, J., Kim, S.Y., Kim, S., 2010. GSA-SNP: A general approach for gene set analysis of polymorphisms. Nucleic Acids Res. 38. https://doi.org/10.1093/nar/gkq428

Nestor, S.M., Rupsingh, R., Borrie, M., Smith, M., Accomazzi, V., Wells, J.L., Fogarty, J., Bartha, R., 2008. Ventricular enlargement as a possible measure of Alzheimer's disease progression validated using the Alzheimer's disease neuroimaging initiative database. Brain 131, 2443–2454. https://doi.org/10.1093/brain/awn146

Pini, L., Pievani, M., Bocchetta, M., Altomare, D., Bosco, P., Cavedo, E., Galluzzi, S., Marizzoni, M., Frisoni, G.B., 2016. Brain atrophy in Alzheimer's Disease and aging. Ageing Res. Rev. 30, 25–48. https://doi.org/10.1016/j.arr.2016.01.002

Potkin, S.G., Turner, J.A., Guffanti, G., Lakatos, A., Torri, F., Keator, D.B., MacCiardi, F., 2009. Genome-wide strategies for discovering genetic influences on cognition and cognitive disorders: Methodological considerations. Cogn. Neuropsychiatry. https://doi.org/10.1080/13546800903059829

Pottier, C., Zhou, X., Perkerson, R.B., Baker, M., Jenkins, G.D., Serie, D.J., Ghidoni, R., Benussi, L., Binetti, G., López de Munain, A., Zulaica, M., Moreno, F., Le Ber, I., Pasquier, F., Hannequin, D., Sánchez-Valle, R., Antonell, A., Lladó, A., Parsons, T.M., Finch, N.C.A., Finger, E.C., Lippa, C.F., Huey, E.D., Neumann, M., Heutink, P., Synofzik, M., Wilke, C., Rissman, R.A., Slawek, J., Sitek, E., Johannsen, P., Nielsen, J.E., Ren, Y., van Blitterswijk, M., DeJesus-Hernandez, M., Christopher, E., Murray, M.E., Bieniek, K.F., Evers, B.M., Ferrari, C., Rollinson, S., Richardson, A., Scarpini, E., Fumagalli, G.G., Padovani, A., Hardy, J., Momeni, P., Ferrari, R., Frangipane, F., Maletta, R., Anfossi, M., Gallo, M., Petrucelli, L., Suh, E.R., Lopez, O.L., Wong, T.H., van Rooij, J.G.J., Seelaar, H., Mead, S., Caselli, R.J., Reiman, E.M., Noel Sabbagh, M., Kjolby, M., Nykjaer, A., Karydas, A.M., Boxer, A.L., Grinberg, L.T., Grafman, J., Spina, S., Oblak, A., Mesulam, M.M., Weintraub, S., Geula, C., Hodges, J.R., Piguet, O., Brooks, W.S., Irwin, D.J., Trojanowski, J.Q., Lee, E.B., Josephs, K.A., Parisi, J.E., Ertekin-Taner, N., Knopman, D.S., Nacmias, B., Piaceri, I., Bagnoli, S., Sorbi, S.,

Gearing, M., Glass, J., Beach, T.G., Black, S.E., Masellis, M., Rogaeva, E., Vonsattel, J.P., Honig, L.S., Kofler, J., Bruni, A.C., Snowden, J., Mann, D., Pickering-Brown, S., Diehl-Schmid, J., Winkelmann, J., Galimberti, D., Graff, C., Öijerstedt, L., Troakes, C., Al-Sarraj, S., Cruchaga, C., Cairns, N.J., Rohrer, J.D., Halliday, G.M., Kwok, J.B., van Swieten, J.C., White, C.L., Ghetti, B., Murell, J.R., Mackenzie, I.R.A., Hsiung, G.Y.R., Borroni, B., Rossi, G., Tagliavini, F., Wszolek, Z.K., Petersen, R.C., Bigio, E.H., Grossman, M., Van Deerlin, V.M., Seeley, W.W., Miller, B.L., Graff-Radford, N.R., Boeve, B.F., Dickson, D.W., Biernacka, J.M., Rademakers, R., 2018. Potential genetic modifiers of disease risk and age at onset in patients with frontotemporal lobar degeneration and GRN mutations: a genome-wide association study. Lancet Neurol. 17, 548–558. https://doi.org/10.1016/S1474-4422(18)30126-1

Power, J., Mayer-Pröschel, M., Smith, J., Noble, M., 2002. Oligodendrocyte precursor cells from different brain regions express divergent properties consistent with the differing time courses of myelination in these regions. Dev. Biol. 245, 362–375. https://doi.org/10.1006/dbio.2002.0610

Purcell, S., Neale, B., Todd-Brown, K., Thomas, L., Ferreira, M.A.R., Bender, D., Maller, J., Sklar, P., de Bakker, P.I.W., Daly, M.J., Sham, P.C., 2007. PLINK: A Tool Set for Whole-Genome Association and Population-Based Linkage Analyses. Am. J. Hum. Genet. 81, 559–575. https://doi.org/10.1086/519795

Querbes, O., Aubry, F., Pariente, J., Lotterie, J.-A., Démonet, J.-F., Duret, V., Puel, M., Berry, I., Fort, J.-C., Celsis, P., 2009. Early diagnosis of Alzheimer's disease using cortical thickness: impact of cognitive reserve. Brain 132, 2036–2047. https://doi.org/10.1093/brain/awp105

Ramanan, V.K., Risacher, S.L., Nho, K., Kim, S., Shen, L., McDonald, B.C., Yoder, K.K., Hutchins, G.D., West, J.D., Tallman, E.F., Gao, S., Foroud, T.M., Farlow, M.R., De

Jager, P.L., Bennett, D.A., Aisen, P.S., Petersen, R.C., Jack, C.R., Toga, A.W., Green, R.C., Jagust, W.J., Weiner, M.W., Saykin, A.J., 2015. GWAS of longitudinal amyloid accumulation on18F-florbetapir PET in Alzheimer's disease implicates microglial activation gene IL1RAP. Brain 138, 3076–3088. https://doi.org/10.1093/brain/awv231

Ramasamy, A., Trabzuni, D., Guelfi, S., Varghese, V., Smith, C., Walker, R., De, T., Coin, L., De Silva, R., Cookson, M.R., Singleton, A.B., Hardy, J., Ryten, M., Weale, M.E., 2014. Genetic variability in the regulation of gene expression in ten regions of the human brain. Nat. Neurosci. 17, 1418–1428. https://doi.org/10.1038/nn.3801

Ridge, P.G., Mukherjee, S., Crane, P.K., Kauwe, J.S.K., 2013. Alzheimer's disease: Analyzing the missing heritability. PLoS One 8, 1–10. https://doi.org/10.1371/journal.pone.0079771

Rogers, J.T., Randall, J.D., Eder, P.S., Huang, X., Bush, A.I., Tanzi, R.E., Venti, A., Payton, S.M., Giordano, T., Nagano, S., Cahill, C.M., Moir, R., Lahiri, D.K., Greig, N., Sarang, S.S., Gullans, S.R., 2002. Alzheimer's disease drug discovery targeted to the APP mRNA 5′untranslated region. J. Mol. Neurosci. 19, 77–82. https://doi.org/10.1007/s12031-002-0014-6

S., C., N., S., E., H., M.M., G., J., B., M., A., D., B., Y., S., 2008. APOE epsilon 4 allele predicts faster cognitive decline in mild Alzheimer disease. Neurology 70, 1842–1849.

Sachdev, P.S., Zhuang, L., Braidy, N., Wen, W., 2013. Is Alzheimer's a disease of the white matter? Curr. Opin. Psychiatry. https://doi.org/10.1097/YCO.0b013e32835ed6e8

Seo, S.W., Im, K., Lee, J.M., Kim, S.T., Ahn, H.J., Go, S.M., Kim, S.H., Na, D.L., 2011. Effects of demographic factors on cortical thickness in Alzheimer's disease. Neurobiol. Aging. https://doi.org/10.1016/j.neurobiolaging.2009.02.004

Serrano-Pozo, A., Frosch, M.P., Masliah, E., Hyman, B.T., 2011. Neuropathological alterations in Alzheimer disease. Cold Spring Harb. Perspect. Med. 1. https://doi.org/10.1101/cshperspect.a006189

Shaw, M.E., Sachdev, P.S., Anstey, K.J., Cherbuin, N., 2016. Age-related cortical thinning in cognitively healthy individuals in their 60s: The PATH Through Life study. Neurobiol. Aging 39, 202–209. https://doi.org/10.1016/j.neurobiolaging.2015.12.009

Sherva, R., Tripodis, Y., Bennett, D.A., Chibnik, L.B., Crane, P.K., De Jager, P.L., Farrer, L.A., Saykin, A.J., Shulman, J.M., Naj, A., Green, R.C., 2014. Genome-wide association study of the rate of cognitive decline in Alzheimer's disease. Alzheimer's Dement. 10, 45–52. https://doi.org/10.1016/j.jalz.2013.01.008

Sled, J.G., Zijdenbos, a P., Evans, a C., 1998. A nonparametric method for automatic correction of intensity nonuniformity in MRI data. IEEE Trans. Med. Imaging 17, 87–97. https://doi.org/10.1109/42.668698

Taoufik, E., Kouroupi, G., Zygogianni, O., Matsas, R., 2018. Synaptic dysfunction in neurodegenerative and neurodevelopmental diseases: An overview of induced pluripotent stem-cell-based disease models. Open Biol. https://doi.org/10.1098/rsob.180138

Teipel, S.J., Bayer, W., Alexander, G.E., Zebuhr, Y., Teichberg, D., Kulic, L., Schapiro, M.B., Möller, H.J., Rapoport, S.I., Hampel, H., 2002. Progression of corpus callosum atrophy in Alzheimer disease. Arch. Neurol. 59, 243–248. https://doi.org/10.1001/archneur.59.2.243

Thal, D.R., Rüb, U., Orantes, M., Braak, H., 2002. Phases of Aβ-deposition in the human brain and its relevance for the development of AD. Neurology 58, 1791–1800. https://doi.org/10.1212/WNL.58.12.1791

Van Der Werf, Y.D., Scheltens, P., Lindeboom, J., Witter, M.P., Uylings, H.B.M., Jolles, J., 2003. Deficits of memory, executive functioning and attention following infarction in the thalamus; a study of 22 cases with localised lesions. Neuropsychologia 41, 1330–1344. https://doi.org/10.1016/S0028-3932(03)00059-9

Verkhratsky, A., Olabarria, M., Noristani, H.N., Yeh, C.Y., Rodriguez, J.J., 2010. Astrocytes in Alzheimer's Disease. Neurotherapeutics 7, 399–412. https://doi.org/10.1016/j.nurt.2010.05.017

Villemagne, V.L., Burnham, S., Bourgeat, P., Brown, B., Ellis, K.A., Salvado, O., Szoeke, C., Macaulay, S.L., Martins, R., Maruff, P., Ames, D., Rowe, C.C., Masters, C.L., 2013. Amyloid β deposition, neurodegeneration, and cognitive decline in sporadic Alzheimer's disease: A prospective cohort study. Lancet Neurol. 12, 357–367. https://doi.org/10.1016/S1474-4422(13)70044-9

Wang, H.F., Wan, Y., Hao, X.K., Cao, L., Zhu, X.C., Jiang, T., Tan, M.S., Tan, Lin, Zhang, D.Q., Tan, Lan, Yu, J.T., 2016. Bridging Integrator 1 (BIN1) Genotypes Mediate Alzheimer's Disease Risk by Altering Neuronal Degeneration. J. Alzheimer's Dis. 52, 179–190. https://doi.org/10.3233/JAD-150972

Waxman, S.G., 1977. Conduction in Myelinated, Unmyelinated, and Demyelinated Fibers. Arch. Neurol. 34, 585–589. https://doi.org/10.1001/archneur.1977.00500220019003

Wilczynska, K.M., Singh, S.K., Adams, B., Bryan, L., Rao, R.R., Valerie, K., Wright, S., Griswold-Prenner, I., Kordula, T., 2009. Nuclear factor i isoforms regulate gene expression during the differentiation of human neural progenitors to astrocytes. Stem Cells 27, 1173–1181. https://doi.org/10.1002/stem.35

Wolthusen, R.P.F., Hass, J., Walton, E., Turner, J.A., Rössner, V., Sponheim, S.R., Ho, B.-C., Holt, D.J., Gollub, R.L., Calhoun, V., Ehrlich, S., 2015. Genetic underpinnings of left

superior temporal gyrus thickness in patients with schizophrenia. World J. Biol.

Psychiatry 2975, 1–11. https://doi.org/10.3109/15622975.2015.1062915

Wong, A.P.Y., French, L., Leonard, G., Perron, M., Pike, G.B., Richer, L., Veillette, S.,

Pausova, Z., Paus, T., 2018. Inter-Regional Variations in Gene Expression and Age-

Related Cortical Thinning in the Adolescent Brain. Cereb. Cortex 28, 1272–1281.

https://doi.org/10.1093/cercor/bhx040

Zhang, B., Gaiteri, C., Bodea, L.G., Wang, Z., McElwee, J., Podtelezhnikov, A.A., Zhang, C.,

Xie, T., Tran, L., Dobrin, R., Fluder, E., Clurman, B., Melquist, S., Narayanan, M.,

Suver, C., Shah, H., Mahajan, M., Gillis, T., Mysore, J., MacDonald, M.E., Lamb, J.R.,

Bennett, D.A., Molony, C., Stone, D.J., Gudnason, V., Myers, A.J., Schadt, E.E.,

Neumann, H., Zhu, J., Emilsson, V., 2013. Integrated systems approach identifies

genetic nodes and networks in late-onset Alzheimer's disease. Cell 153, 707–720.

https://doi.org/10.1016/j.cell.2013.03.030

Zhang, Y., Chen, K., Sloan, S.A., Bennett, M.L., Scholze, A.R., O'Keeffe, S., Phatnani, H.P.,

Guarnieri, P., Caneda, C., Ruderisch, N., Deng, S., Liddelow, S.A., Zhang, C., Daneman,

R., Maniatis, T., Barres, B.A., Wu, J.Q., 2014. An RNA-Sequencing Transcriptome and

Splicing Database of Glia, Neurons, and Vascular Cells of the Cerebral Cortex. J.

Neurosci. 34, 11929–11947. https://doi.org/10.1523/jneurosci.1860-14.2014

Zhang, Y., Sloan, S.A., Clarke, L.E., Caneda, C., Plaza, C.A., Blumenthal, P.D., Vogel, H.,

Steinberg, G.K., Edwards, M.S.B., Li, G., Duncan, J.A., Cheshier, S.H., Shuer, L.M.,

Chang, E.F., Grant, G.A., Gephart, M.G.H., Barres, B.A., 2016. Purification and

Characterization of Progenitor and Mature Human Astrocytes Reveals Transcriptional

and Functional Differences with Mouse. Neuron 89, 37–53.

https://doi.org/10.1016/j.neuron.2015.11.013

Zijdenbos, A., Evans, A., Riahi, F., Sled, J., Chui, J., Kollokian, V., 1996. Automatic

quantification of multiple sclerosis lesion volume using stereotaxic space. Vis. Biomed.

Comput. 1131, 439–448.
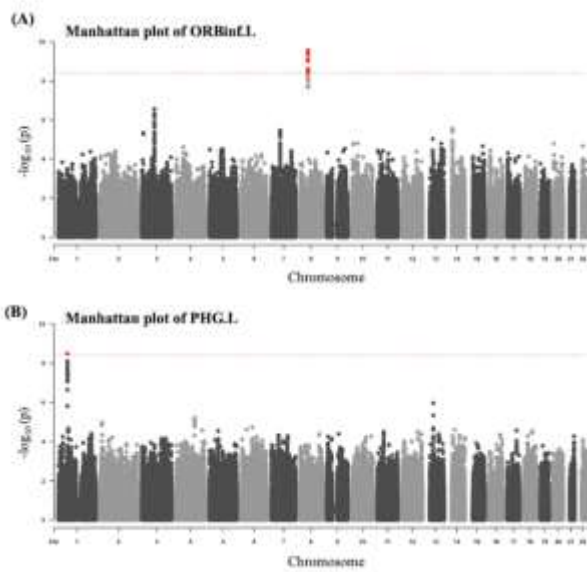
Figure Legends

Figure 1. Manhattan plots for GWAS of mean cortical thickness. Manhattan plot for mean cortical thickness in the (A) left inferior frontal gyrus (orbital part) (ORBinf.L) and (B) left parahippocampal gyrus (PHG.L). The horizontal axis (x-axis) shows the base pair position of each SNP on the autosomal chromosome, and the vertical axis (y-axis) shows the observed –log10(p-values) for the association. The red horizontal line indicates genome-wide significant threshold (p-value $< 4.17 \times 10^{-9}$), and significant SNPs are colored in red.
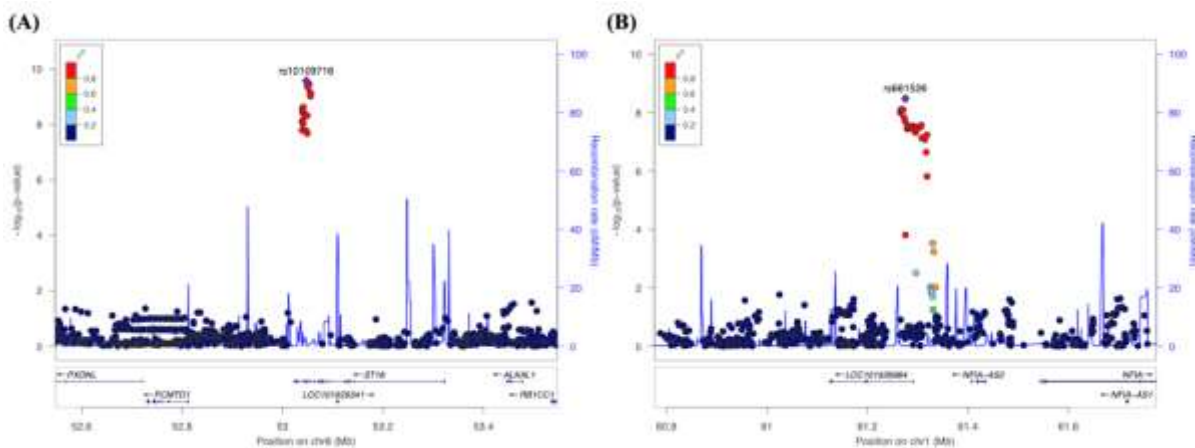
Figure 2. Regional association plots for GWAS of mean cortical thickness. All SNPs within 500 kb upstream and downstream of rs10109716 on chromosome 8 (A) and rs661526 on chromosome 1 (B) are plotted based on their GWAS $-\log_{10}$(p-values) of ORBinf.L and PHG.L, respectively. The most significant SNP is highlighted in violet. The color scale of r^2 values is used to label SNPs based on their degree of linkage disequilibrium with rs10109716 and rs661526, respectively. Genes in the region are labeled with arrows denoting the 5'–3' orientation. All plots were adapted from LocusZoom results.
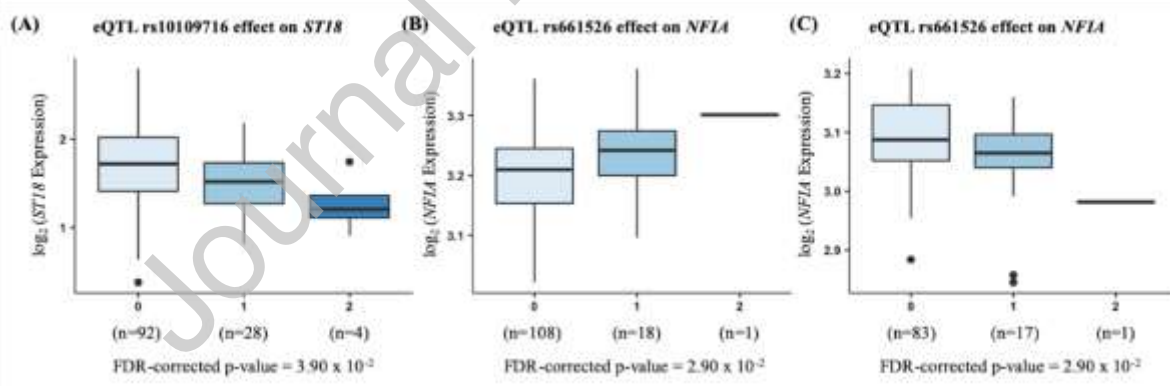

Figure 3. Effect of rs10109716 and rs661526 on ST18 and NFIA expression. Expression quantitative trait loci (eQTL) box plots of association between genotypes of rs10109716 with ST18 in thalamus (A) and rs661526 with NFIA in frontal cortex (B) and substantia nigra (C). The x-axes correspond to the SNP genotype, and the y-axes represent the log2 gene expression values.

Tables

Table 1. Demographic information for 919 ADNI participants

	ADNI-1 (n=592)	**ADNI-GO/2 (n=327)**
Age (years) (mean ± s.d.)	75.59 ± 6.56	72.99 ± 7.18
Sex (male/female)	358 / 234	183 / 144
Education (years) (mean ± s.d.)	15.67 ± 3.00	16.16 ± 2.66
Diagnosis (AD/MCI/CN)	139 / 286 / 167	24 / 202 / 101
APOE ε4 (0/1/2 copies)	295 / 231 /66	194 / 109 /24

AD: Alzheimer's disease; MCI: mild cognitive impairment; CN: cognitively normal controls; *APOE* ε4 represents the number of ε4 copies in rs429358 and rs7412 single nucleotide polymorphism (SNPs).

Table 2. Comparison of selected cortical thicknesses between different disease groups

Abbreviation	Region	Disease Status			P-value
		AD	MCI	CN	
IFGoperc.L	Left Inferior frontal gyrus, opercular part	3.14 (0.16)	3.19 (0.13)	3.21 (0.14)	1.46E-06
IFGtriang.L	Left Inferior frontal gyrus, triangular part	3.04 (0.17)	3.11 (0.14)	3.13 (0.13)	8.84E-09
ORBinf.L	Left Inferior frontal gyrus, orbital part	3.24 (0.16)	3.33 (0.16)	3.35 (0.14)	5.84E-12
ORBsupmed.L	Left Superior frontal gyrus, medial orbital	3.08 (0.19)	3.17 (0.18)	3.18 (0.17)	5.47E-07
ORBsupmed.R	Right Superior frontal gyrus, medial orbital	3.14 (0.21)	3.21 (0.19)	3.22 (0.16)	1.48E-05
ACG.L	Left Anterior cingulate and paracingulate gyri	3.07 (0.18)	3.12 (0.17)	3.13 (0.18)	6.77E-04
ACG.R	Right Anterior cingulate and paracingulate gyri	3.11 (0.17)	3.13 (0.17)	3.13 (0.17)	2.33E-01
PCG.L	Left Posterior cingulate gyrus	3.11 (0.21)	3.25 (0.21)	3.29 (0.18)	2.56E-20
PCG.R	Right Posterior cingulate gyrus	3.10 (0.23)	3.26 (0.21)	3.30 (0.20)	3.76E-24
PHG.L	Left Parahippocampal gyrus	2.93 (0.19)	3.07 (0.19)	3.15 (0.16)	1.41E-36
PHG.R	Right Parahippocampal gyrus	2.95 (0.20)	3.10 (0.20)	3.17 (0.16)	2.31E-33
STG.L	Left Superior temporal gyrus	3.11 (0.17)	3.25 (0.16)	3.29 (0.12)	7.76E-30
STG.R	Right Superior temporal gyrus	3.16 (0.18)	3.28 (0.16)	3.33 (0.13)	2.10E-28
TPOmid.L	Left Temporal pole: middle temporal gyrus	3.71 (0.31)	3.87 (0.26)	3.92 (0.24)	1.29E-15
TPOmid.R	Right Temporal pole: middle temporal gyrus	3.72 (0.29)	3.87 (0.27)	3.92 (0.23)	1.39E-13
ITG.L	Left Inferior temporal gyrus	3.31 (0.25)	3.47 (0.19)	3.53 (0.17)	5.31E-25
ITG.R	Right Inferior temporal gyrus	3.36 (0.27)	3.51 (0.20)	3.56 (0.18)	7.81E-20

Mean cortical thickness (mm) and standard deviation of 17 selected ROIs and difference of adjusted thickness between three groups.

AD: Alzheimer's Disease, MCI: Mild Cognitive Impairment, CN: Cognitive Normal. P-value: FDR-corrected p-value

Table 3. Results of differential expression analyses of cortical thickness associated genes

Gene	Chromosome	Brain Tissues	log$_2$FC	t	P-value
NFIA	1	Left hippocampus	0.141	1.786	0.083
		Right hippocampus	0.093	2.262	**0.027**
		Left parietal cortex	0.001	0.009	0.993
		Right parietal cortex	0.027	0.586	0.560
		Left temporal cortex	-0.027	-0.276	0.784
		Right temporal cortex	0.041	0.925	0.358
ST18	8	Left hippocampus	0.097	0.712	0.482
		Right hippocampus	-0.031	-0.453	0.652
		Left parietal cortex	-0.016	-0.058	0.954
		Right parietal cortex	-0.679	-1.128	0.264
		Left temporal cortex	-0.117	-0.539	0.594
		Right temporal cortex	0.320	2.273	**0.026**

Differentially expressed results with p-value < 0.05 are indicated in bold in the table